# On Modeling the RIS as a Resource: Multi-User Allocation and Efficiency-Proportional Pricing

Alexandros Papadopoulos, Dimitrios Tyrovolas, *Member, IEEE*, Antonios Lalas, Konstantinos Votis, Stefan Schmid, Sotiris Ioannidis, George K. Karagiannidis, *Fellow, IEEE*, and Christos K. Liaskos

***Abstract*—Programmable Wireless Environments aim to render the communication environment a controllable, software-defined medium. Reconfigurable Intelligent Surfaces (RISes) are the key enabling technology, which can offer the real-time capability to manipulate impinging waves. RISes are expected to be widely deployed in B5G/6G networks to serve a large number of users simultaneously. Despite numerous analyses highlighting the benefits of utilizing previously unexploitable propagation factors through the use of RISes, there is a lack of analysis regarding their relation to the concept of network resource, their allocation to users/stakeholders and their fair pricing. Thus, this paper models RISes as networked resources. Based on this definition, the PRIME algorithm is proposed, the first algorithm for RIS resource allocation and joint pricing. PRIME strives for proportionality between the offered end-user performance level and the corresponding resource pricing, promoting fairness. The algorithm is validated via full-wave electromagnetic simulations and applies to multiple RIS functionalities and frequency bands.**

***Index Terms*—RIS, resource allocation, multiplexing, pricing.**

Received 21 August 2024; revised 24 February 2025; accepted 26 May 2025. Date of publication 2 June 2025; date of current version 7 October 2025. This work was funded by the SNS JU under the EU Horizon Europe research and innovation program through the NATWORK project (Grant No. 101139285), the German Federal Ministry of Education and Research (BMBF) under Grant 16KISK020K (6G-RIC, 2021-2025), and the WISAR and 6G-RIC projects. The associate editor coordinating the review of this article and approving it for publication was M. Reisslein. *(Corresponding author: Alexandros Papadopoulos.)*

Alexandros Papadopoulos is with the Computer Science Engineering Department, University of Ioannina, 45110 Ioannina, Greece, and also with the Information Technologies Institute, CERTH, 57001 Thessaloniki, Greece (e-mail: a.papadopoulos@uoi.gr/alexpap@iti.gr).

Dimitrios Tyrovolas is with the Department of Electrical and Computer Engineering, Aristotle University of Thessaloniki, 54124 Thessaloniki, Greece (e-mail: tyrovolas@auth.gr).

Antonios Lalas and Konstantinos Votis are with the Information Technologies Institute, CERTH, 57001 Thessaloniki, Greece (e-mail: lalas@iti.gr; kvotis@iti.gr).

Stefan Schmid is with the Department of Computer Science, TU Berlin, 10623 Berlin, Germany, and also with the Department of Secure Information Technology of Fraunhofer, Fraunhofer SIT, 64295 Berlin, Germany (e-mail: stefan.schmid@tu-berlin.de).

Sotiris Ioannidis is with the Department of Electrical and Computer Engineering, Technical University of Crete, 70013 Heraklion, Greece (e-mail: sotiris@ece.tuc.gr).

George K. Karagiannidis is with the Department of Electrical Engineering, Taif University, Taif 21944, Saudi Arabia, and also with the Department of Electrical and Computer Engineering, Aristotle University of Thessaloniki, 54124 Thessaloniki, Greece (e-mail: geokarag@auth.gr).

Christos K. Liaskos is with the Computer Science Engineering Department, University of Ioannina, 45110 Ioannina, Greece, and also with the Institute of Computer Science, Foundation for Research and Technology Hellas (FORTH), 70013 Heraklion, Greece (e-mail: cliaskos@uoi.gr).

Digital Object Identifier 10.1109/TNSM.2025.3576038

## I. Introduction

THE ADVENT of new technologies towards Beyond-5G (B5G) and 6G wireless communications has fundamentally changed our perception of future communication paradigms. Until now, the propagation environment has been considered a given and uncontrollable factor, with phenomena such as fading and scattering being treated stochastically. However, in new wireless technologies, the environment is viewed as a set of programmable resources that can be optimally configured, transforming the entire system setting into a Programmable Wireless Environments (PWE) [1].

The main technology driving this transformation are the Reconfigurable Intelligent Surfaces (RISes). An RIS can interact with impinging electromagnetic (EM) waves in real-time and in a software-defined manner [2]. This interaction aims to effectively utilize previously uncontrollable resources, such as the scattering behavior of passive objects, significantly improving the Quality of Service (QoS) for users.

At the system level, PWEs are created by coating all planar surfaces within an area with RISes. Each separate RIS can then be programmed in terms of its interaction with impinging waves, e.g., creating cascading paths and reaching non-line-of-sight areas (nLos). In this context, the EM propagation within a space can be dynamically manipulated, benefiting the users in real-time [1].

As noted, the most characteristic feature of PWEs is their capability to reconstruct LoS channels between base stations and users. However, this is not the most challenging feature of PWEs. Signals can also be kept away from specific areas, creating "quiet zones" within the network and enhancing its physical security [3]. Additionally, PWEs can enhance safety through improved object detection and localization features [4]. Lastly, the significant impact of the Doppler effect [5], especially in Vehicle-to-Everything (V2X) communication links, can be mitigated by ensuring the direction of arrival of signal remains perpendicular to the trajectory of a mobile user.

Within the PWE, as with almost any other components in a communication network, each RIS unit will need to simultaneously serve multiple users with different requirements. In networking terms, each RIS is a resource that should be shareable among users. The definition of the RIS-as-a-resource, and its efficient allocation across multiple users should be clearly described, in order to be integrated to the policy of the stakeholder managing the infrastructure containing the PWE.

TABLE I
LIST OF ABBREVIATIONS

| Abbreviation | Definition |
|---|---|
| AI | Artificial Intelligence |
| B5G | Beyond-5G |
| BS | Base Station |
| CC | Common RIS Configuration |
| CE | Codebook Entry |
| CPU | Central Processing Unit |
| EM | Electromagnetic |
| IoT | Internet of Things |
| LoS | Line of Sight |
| MEMS | Micro-Electro-Mechanical Systems |
| nLoS | Non-Line of Sight |
| NSGA-II | Non-dominated Sorting Genetic Algorithm II |
| PF | Payment Factor |
| PICCS | Physics Informed Codebook Compilation Software |
| PWE | Programmable Wireless Environments |
| RAN | Radio Access Network |
| RIS | Reconfigurable Intelligent Surface |
| RL | Reinforcement Learning |
| S21 | Transmission Coefficient |
| TDMA | Time-Division Multiple Access |
| UE | User Equipment |
| V2X | Vehicle to Everything |
| VNF | Virtual Network Function |
| VPM | Virtual Programmable Metasurface |

The transformation of well-established resource allocation strategies in already existing technologies [6] can boost the same procedures in the context of PWEs. One such strategy is the division of a RIS unit into multiple virtual ones [7]. Beyond existing knowledge, dedicated frameworks for serving multiple users with RIS have already been proposed and discussed [8]. Nonetheless, a gap exists in the precise manner in which the RIS resource will be defined and be allocated to network users in accordance with their pricing levels, in accordance with their service-level agreements.

In this context, our research contributions are as follows:

- We define the notion of RIS as a networked system resource.
- Subsequently, we present the first resource allocation algorithm, aligned to our resource definition. The algorithm supports multiple RIS functionality types and can be adapted to any pricing policy. A fair pricing policy is provided as a default.
- We evaluate the algorithm's efficiency via realistic, full-wave EM simulations. Moreover, we deduce the computational complexity of the algorithm, noting its applicability to real-world scenarios.

The rest of this paper is organized as follows: Section II provides the prerequisite knowledge. Section III presents the related studies. Section IV defines the notion of RIS as a networked resource, while Section V elaborates on the resource allocation algorithm proposed in this paper. The evaluation of the algorithm is presented in Section VI. Section VII discusses potential research challenges, and Section VIII offers conclusions.

## II. PREREQUISITES

The RIS technology is based on the principles of metamaterials, which are artificially engineered structures created by connecting basic units known as unit cells. From a macroscopic perspective, a RIS appears as a thin, planar, and rectangular device, resembling a tile, composed of an array of these unit cells. Within these tiles, various active elements [9], such as PIN diodes or MEMS [10], are embedded. Controlling these active elements enables the RIS to manipulate impinging EM waves propagation across its surface in a software-defined manner.

Specifically, when an EM wave impinges on the RIS surface, it induces a specific current distribution. This distribution is strongly connected with the state of all of its active elements, which is referred to as the RIS *configuration*. By properly determining the RIS configuration, the incident EM wave can be effectively manipulated, leading to various macroscopic responses, known as RIS *functionalities*. These include beam steering, beam splitting, perfect absorption, modulation of the wavefront's phase, amplitude, and/or polarization, as well as wavefront sensing [11].

Defining the optimal RIS configuration for a specific functionality is a complex and time-consuming optimization task [12]. Therefore, it is not usually feasible to compute this during the RIS operation phase. Instead, this task is completed during the manufacturing phase. During this phase, the functionalities supported by the RIS unit are matched with the optimal RIS configuration by combining knowledge gained from physics insights and metaheuristic tools, within a simulation tool or prototyped measurement system [12]. These mappings are saved in a Codebook Database. Consequently, once the RIS is in the operation phase and needs to achieve a specific functionality, it only needs to retrieve the corresponding entry from the codebook [1].

The RIS technology is towards its integration into current communication networks. Thus, it will soon need robust mechanisms to serve multiple users simultaneously. The most efficient and straightforward way to make real-time serving of multiple users feasible is through the multiplexing of codebook entries [13]. This means that multiple users share the RIS elements, whose values are determined based on all the respective codebook entries.

An algorithm that can efficiently multiplex the codebook entries is COMMON [13], [14]. The COMMON algorithm retrieves the codebook entries for the users from the respective database, pre-processes them, and then sets each RIS element to the most frequent value among the codebook entries resulting to the final, common RIS configuration. Its workflow is presented in Alg. 1.

The RIS resource allocation procedure, in addition to the definition of the common RIS configuration, also requires a pricing mechanism to ensure that the sharing of RIS elements leads to the proper distribution of the resources to each user. Since COMMON lacks such a mechanism, in this paper, we introduce the PRIME algorithm (Section V).

## III. RELATED WORK

Dynamic resource allocation in wireless networks is a widely studied topic in research literature. The primary objectives are to ensure fair satisfaction for a dynamically changing

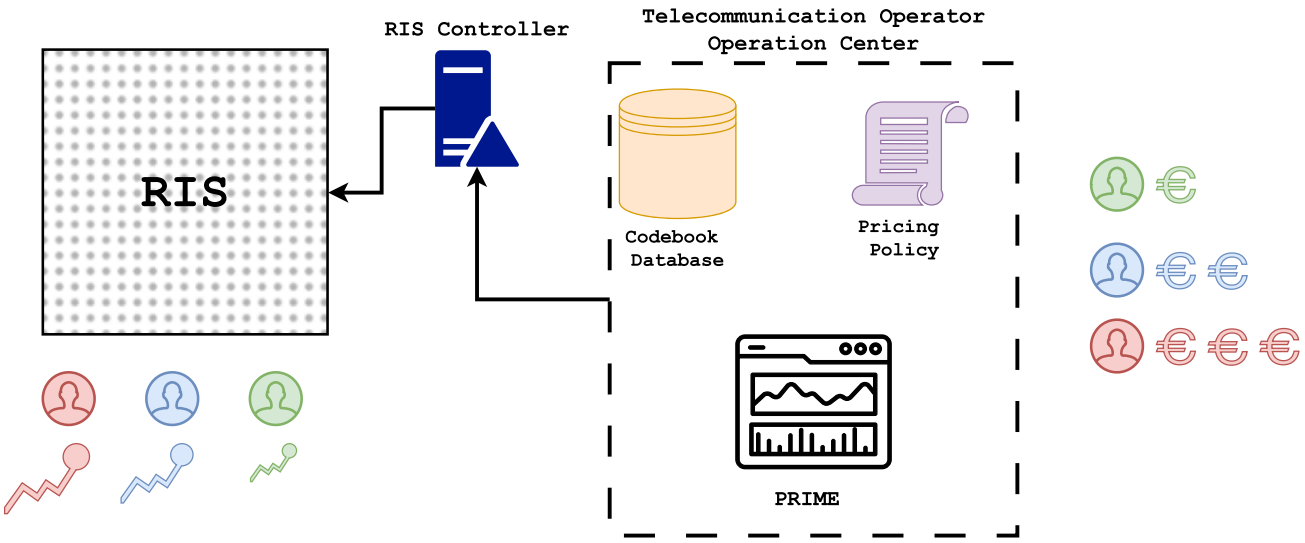


Fig. 1. The resource allocation procedure in a RIS-assisted environment with the integration of PRIME algorithm.

**Algorithm 1:** Codebook Multiplexing Algorithm (COMMON)

**Input:** Dimensions of RIS ($M$, $N$), Number of users $K$, discretization parameter $N_d$, Codebook Entries $CE_k$
**Output:** Common RIS configuration $CC(M, N)$
*Initialization*: Discrete Entries $DE_k$
*Discretization function* $f_{dis}(N_d)$*:*
**for** $k = 1$ to $K$ **do**
  $DE_k \leftarrow f_{dis}(CE_k, N_d)$
**end for**
Initialize $CC(M, N)$ to store the final RIS configuration
**for** each element ($m$, $n$) in $CC$ **do**
  Initialize an empty list *values*
  **for** $k = 1$ to $K$ **do**
    Append $DE_k(m, n)$ to *values*
  **end for**
  *Determine each element value with the most frequent one*
  $CC(m, n) \leftarrow \text{ComputeMostFrequent}(values)$
**end for**
**return** $CC$

number of users [6] and to manage network resources according to specific parameters, such as energy and bandwidth constraints [15].

Two prominent methods for resource allocation are network slicing and virtual switching. Network slicing involves partitioning network resources to meet the specific requirements of individual users. For example, [16] introduces a radio access network (RAN) slicing technique that employs deep reinforcement learning (RL) to flexibly allocate RAN resources. When network resources are limited, [17] addresses the challenge of fairly distributing multiple resources by proposing an optimization framework based on the Ordered Weighted Average operator. Additionally, [18] presents a machine learning-based RAN slicing strategy that utilizes AI models to maximize spectrum efficiency and maintain service satisfaction levels despite user mobility.

As concerns virtual switching, it has emerged as a critical technique for resource allocation and network slicing by virtualizing the core network to serve different users. In [19], the authors propose an iterative optimization framework for allocating resources among the network owner, cloud owner, and slice network owner to achieve optimal bandwidth distribution. Furthermore, [20] discusses the optimal placement of Virtual Network Functions (VNFs) within a physical network, considering deployment costs and resource consumption, and offers solutions for multi-hop networks with bandwidth limitations and scalability concerns. Building on this approach, [7] introduces the concept of a Virtual Programmable Metasurface (VPM), analogous to Virtual Machines. VPMs are designed as software entities that encapsulate specific subsets of the RIS physical elements, simplifying their management and control.

Optimization of RIS-assisted networks has been approached using AI and game theory. In [21], authors apply RL to optimize both base station transmit power and RIS configurations, improving performance and energy efficiency. In [22], deep RL is used for spectrum allocation in RIS-enabled V2X networks, enabling intelligent spectrum management in dynamic environments. Meanwhile, authors in [23] use game theory to maximize data rates in heterogeneous cellular networks with RIS by modeling interactions as a coalition game for optimal resource allocation.

The PWE concept requires multiple RIS units within the communication network, necessitating the simultaneous allocation of their resources. In [2], multiple RIS are managed through an external software service that calculates and deploys the optimal interaction configurations for each unit to best meet user needs. Building on this concept, authors in [24] proposed a two-stage RL-based solution aimed at maximizing energy efficiency while minimizing latency.

To the best of the authors' knowledge, existing resource allocation strategies for RIS-assisted environments that utilize

learning-based methods and game theory primarily focus on optimizing network parameters to achieve overall performance improvements. However, allocating these resources among users with different pricing levels within RIS-assisted networks remains a significant challenge, as the current frameworks addressing this task are notably limited.

In [8], a resource-sharing model for PWE is introduced. The primary concept involves the concurrent provision of multiple functionalities through the segmentation of each RIS. Each RIS tile or group of tiles is assigned to specific tasks. The proposed algorithm then allocates competing user requests based on weighted policies, ensuring a Time-Division-Multiple-Access (TDMA) style of resource sharing in the PWE. Similarly, in [25], RIS multi-tasking involves the use of time duty-cycling, where each user is allocated specific time slots during which they are served by a RIS unit.

It is essential to consider that the RIS unit manages the desired manipulation of EM waves due to its total area. Splitting the RIS into multiple segments may lead to lower performance for all users. As for TDMA, this method requires stringent synchronization. Additionally, latency due to the alignment of the elements' values at the hardware level with the desired values in each time-frame must be considered. Furthermore, due to the nature of TDMA, when a specific user is served by the RIS unit, no gains are achieved for the remaining users.

In contrast, in our previous work [13], we proposed the COMMON algorithm, which is presented here as Alg. 1. This algorithm efficiently multiplexes the RIS configurations of each user into a common one, thereby enabling the concurrent serving of multiple users.

However, COMMON cannot allocate the resources of the RIS-assisted network in multiple users with different pricing levels. For this reason, we propose PRIME, the first algorithm for this purpose. As depicted in Fig. 1, PRIME is integrated into the Telecommunication Stakeholder Operation Center. Users participate in the network based on the defined pricing policy, and the supported RIS functionalities are available as codebook entries in the dedicated database. PRIME's objective is to effectively combine these two components.

The PRIME algorithm determines the common RIS configuration by allocating its elements according to each user's pricing policy. This configuration is then sent to the RIS controller to ensure proper alignment of the microscopic RIS state. Users with higher pricing levels have a greater influence on the RIS configuration, ensuring a proportional relationship between user performance and pricing level. Additionally, PRIME can be implemented in cascaded RIS links.

## IV. Definition of RIS as Network Resource

In order to define the notion of the RIS resource, we employ the notion of EM functions [26]. As noted, these are macroscopic descriptors of the manipulation exerted by the RIS to the impinging wave. They are expressed in software terms, i.e., as functions with well-defined input and output data.

For instance, the $\texttt{PLANAR\_ABSORB}(\overrightarrow{r}) \rightarrow \emptyset$ function describes the full absorption of a planar wave impinging on the RIS from a direction $\overrightarrow{r}$. The $\texttt{PLANAR\_STEER}(\overrightarrow{r}) \rightarrow \overrightarrow{d}$ describes the reflection or refraction of a wave impinging from direction $\overrightarrow{r}$ to direction $\overrightarrow{d}$. The $\texttt{PLANAR\_SPLIT}(\overrightarrow{r}) \rightarrow [\{\overrightarrow{d_1}, p_1\}, \dots]$ described the reflection or refraction of the impinging wave into a set of different directions, $\overrightarrow{d}_i$, each carrying a portion, $p_i$, of the power of the original, impinging wave. Notice that function, $f$, must have a corresponding set of RIS element states, $\sigma_{ij}$, such that $\sigma_{ij} \rightarrow f$. In other words, setting the RIS elements to the states $\sigma_{ij}$ yields the macroscopic function $f$. The definition of $\sigma_{ij}$ depends on the RIS design and can be, e.g., cell phases, cell impedances, or even voltages applied to embedded actuators.

The above EM function examples are ideal in terms of performance. In practice, each has a degree of efficiency, $\epsilon$, when implemented, e.g., due to material losses, RIS design specifications or RIS multitasking (i.e., serving two or more EM functions at the same time). Extending the notation, we can exemplary write $\texttt{PLANAR\_ABSORB}(\overrightarrow{r}) \rightarrow \epsilon$, and $\epsilon$:$\texttt{PLANAR\_STEER}(\overrightarrow{r}) \rightarrow \overrightarrow{d}$. The definition of $\epsilon$ can be adapted depending on the set system specifications. E.g., for $\texttt{PLANAR\_ABSORB}(\overrightarrow{r})$, it can be defined as either the maximum reflected or refracted power towards any direction, or as the attenuation degree of the impinging wave. For $\texttt{PLANAR\_STEER}$ it can be defined as the gain towards the intended direction of departure, the ratio of power towards $\overrightarrow{d}$ divided by the total reradiated power, etc.

Complimenting the requirements for defining the RIS resource notion, note that a RIS has been shown to be able to serve many EM functions simultaneously [13]. In particular, for a set of functions $\epsilon_1 : f_1 \rightarrow \sigma_{ij}^{(1)}$, ..., $\epsilon_k : f_k \rightarrow \sigma_{ij}^{(k)}$, ..., $\epsilon_n : f_n \rightarrow \sigma_{ij}^{(n)}$, there exists a single $\sigma_{ij} : \sigma_{ij}(\sigma_{ij}^{(1)}, \dots, \sigma_{ij}^{(k)}, \dots \sigma_{ij}^{(n)})$ such that:

$$\sigma_{ij} \rightarrow \{\epsilon_1' : f_1, \dots, \epsilon_k' : f_k, \dots, \epsilon_n' : f_n\}. \tag{1}$$

Notice that the merging of $\sigma_{ij}^{(1)}, \dots, \sigma_{ij}^{(k)}, \dots \sigma_{ij}^{(n)}$ into $\sigma_{ij}$ yields the same functions, but alters the efficiency of each.

With the above definitions, we proceed to define the notion of the RIS resource, by first drawing a parallelism to a more common and well-understood resource, the CPU. A CPU is a resource shared by applications. When a single application is running on a CPU, it is allotted the full number of clock ticks per second that the specific CPU can offer. When a number of additional applications is running on the same CPU, the original application gets a reduced number of clock ticks. The resource slice is the ratio of the new allotted clock ticks, divided by the full number of clock ticks allotted when ran alone on the CPU.

Based on the above, we define the following:

*Definition 1:* A RIS is a resource that is shared by macroscopic EM functions.

Moreover:

*Definition 2:* The resource slice allotted to an EM function, $f$, is defined as the ratio $r$ such that

$$r_f = \frac{\epsilon'}{\epsilon} \tag{2}$$

where $\epsilon$ is the efficiency of $f$ when hosted alone on the RIS, and $\epsilon'$ is its efficiency when hosted with other EM functions on the same RIS, $\sigma_{ij} \rightarrow \{\epsilon' : f, \ldots, \epsilon'_k : f_k, \ldots, \epsilon'_n : f_n\}$.

## V. PRIME: A Novel Algorithm Scheme for Sharing & Pricing

In this section, we present the PRIcing-based Multiplexing of codebook Entries (PRIME) algorithm. PRIME, mainly, is dedicated to the definition of $r_f$ factor of Eq. (2) and its workflow is presented in Alg. 2. It is designed for allocation of the RIS resources via the pricing-based multiplexing of codebook entries. PRIME ensures that each user's performance reflects their pricing level.

The required inputs for the algorithm include the dimensions of the RIS (*M*, *N*), the total number of users *K* utilizing the RIS unit for enhanced performance within the communication network, and a discretization parameter $N_d$. Additionally, the algorithm must have access to the Codebook Database, which contains the entries for the optimal RIS configuration for each user. It is important to note that the computation of these codebook entries is not part of the algorithm and is assumed to be an input.

The adaptation of the PRIME algorithm to existing stakeholder pricing policies is achieved through the definition of the Payment Factor (PF). The PF is a positive integer assigned to each user upon entering the resource allocation process. Stakeholders can define multiple discrete PF values, assigning them in a way that quantitatively reflects the varying levels of performance granted to users based on their pricing tiers. This approach accommodates heterogeneous user demands and requirements by ensuring that users with higher PFs receive proportionally greater influence in the allocation process. All users' PFs must be provided as input to the algorithm to accurately incorporate these pricing levels into the resource allocation mechanism.

PRIME begins by retrieving the codebook entries, *CE*, matching the user requests for a RIS functionality. Next, it discretizes all the elements of *CE* based on the discretization parameter $N_d$ leading to the *DE* matrices. Using the PF values, the algorithm then creates an equal number of replicas for each $DE_k$, which is why PFs must be natural numbers. After generating all the replicas of the discretized values, the algorithm determines the common RIS configuration, *CC*, by selecting the most frequent values among the replicas for each RIS element. As is evident, users with higher PF values have a greater influence on the *CC* due to the increased number of replicas of their entries that participate in the final selection, ensuring the pricing part of the PRIME.

The evaluation of the algorithm's feasibility in real-world applications is closely tied to the computational time required for pricing-based codebook entries multiplexing.

**Algorithm 2:** PRIcing-Based Multiplexing of Codebook Entries (PRIME)

**Input:** Dimensions of RIS (*M*, *N*), Number of users *K*, discretization parameter $N_d$, Codebook Entries $CE_k$, Payment Factors $PF_k$
**Output:** Common RIS configuration $CC(M, N)$
*Initialization*: Discretize $CE_k$ to $DE_k$
*Discretization function* $f_{dis}(N_d)$*:*
**for** $k = 1$ to *K* **do**
  $DE_k \leftarrow f_{dis}(CE_k, N_d)$
**end for**
*Replica Creation based on Payment Factors*:
Initialize an empty list *replicas*
**for** $k = 1$ to *K* **do**
  Append $DE_k$ to $PF_k$ *replicas*
**end for**
Initialize $CC(M, N)$ to store the final RIS configuration
*Determine each element value with the most frequent one*
**for** each element (*m*, *n*) in *CC* **do**
  $CC(m, n) \leftarrow \text{ComputeMostFrequent}(replicas)$
**end for**
**return** *CC*

Analyzing the algorithm's workflow, the computational complexity depends on PF values, the dimensions of the RIS unit, and the total number of users.

First, the algorithm discretizes the codebook entries for each user across the RIS elements, resulting in a computational complexity of $O(KMN)$. Next, the algorithm generates configuration replicas based on each user's PF values, adding another layer of complexity. These replicas are then combined, resulting in a computational complexity proportional to the number of users and their respective PFs. Consequently, this part of the algorithm incurs a complexity equivalent to the sum of all PF values, denoted as $O(\sum PF)$. Therefore, the overall computational complexity of the PRIME algorithm is expressed as $O(KMN + \sum PF)$.

## VI. Evaluation

In this section, the PRIME algorithm is evaluated using full-wave EM simulations. We investigate the critical relationship between each user's received performance and their respective PF. A novel efficiency metric is defined, allowing for the comparison of PRIME with alternative approaches. Finally, PRIME is evaluated in multiple RIS-assisted networks.

### A. PRIME Application Based on Full-Wave EM Simulations

First, we assess the capability of the PRIME algorithm to efficiently allocate the RIS elements according to each user's pricing level, as expressed by the PF. The evaluation is conducted using full-wave EM simulations. In the following, we present the evaluation setup, the application of PRIME algorithm and a discussion of the main conclusions.

*1) System Model:* The communication network consists of 4 different base stations. The total number of users are 5 and there is one RIS unit. To encompass a more general concept, two users are served by the same base station, while the remaining three are served by different ones.

*2) Scenario:* The LoS connection between the users and their respective base stations is blocked. The users are positioned opposite a RIS unit with the goal of restoring the LoS connection. The RIS unit elements are shared among the five users. The resource allocation is established via a PF assigned to each user. Each user's PF is unique.

*3) Physical Layer:* The RIS unit used during the full-wave EM simulations has been introduced in our previous work [12]. In this design, depicted in Fig. 2, the RIS unit cells consist of gaps between square metal patches, bridged by lumped complex impedance loads. These patches are positioned on a metal-backed dielectric substrate and a thin metal sheet that serves as a ground plane. Specifically, the substrate is Rogers RT/Duroid 5880, which has an electric permittivity, $\varepsilon_r$, of 2.2, a tangent loss, $\tan\delta$, of 0.0009, and a thickness of 1.016 mm. The ground plane, like the square patches, is a perfect conductor with a thickness of 17.5 μm. There are 6 square patches on the y-axis and 12 on the x-axis. The number of tunable loads is 66. This cell design eliminates transmission and offers wide angular and spectral bandwidth. The value of its embedded load allows control over the amplitude and phase of the reflected wave in the $x$ polarization.

*4) Metrics of Performance:* The EM energy flow between the base station $(BS)$ and the user equipment $(UE)$ is estimated using the $S_{21}$ parameter [27]. The $S_{21}$ parameter, also known as the transmission coefficient, measures the signal transmission from port 1 to port 2 in a network. Essentially, it quantifies the proportion of the signal that successfully travels from the input port to the output port, providing a clear indication of the signal's efficiency as it propagates through the system. In our case, we compute the $S_{21}$ parameter between each user and their respective base station. When the transmission coefficient is very low, it indicates that the LoS path between the *BS* and the *UE* is blocked. By strategically placing the RIS, we aim to establish an alternative communication pathway from the *BS* to the *UE* via the RIS. Through the optimization of RIS configuration, we can effectively maximize the $S_{21}$ parameter, thereby improving overall network performance and user experience in dynamic and obstructed environments.

*5) Tools & Creation of The Codebook Database:* The full-wave EM simulations that are utilized for the evaluation of the PRIME algorithm have been conducted via measurements in an open solver called openEMS [28]. (For the remainder, "measurements" refer to full-wave EM simulation results.)

As mentioned previously, only the pricing-based multiplexing, not the computation of the codebook entries, is part of the PRIME algorithm. Therefore, the optimal RIS configuration for each user when served individually by the RIS must be measured and saved in the Codebook Dataset. For this procedure, we use the Physics Informed Codebook Compilation Software (PICCS) introduced in [12]. PICCS combines physics insights with metaheuristic tools. In our

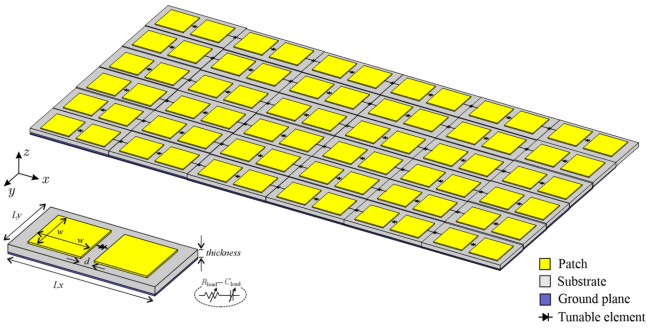


Fig. 2. The design of the RIS unit used in EM measurements for PRIME evaluation.

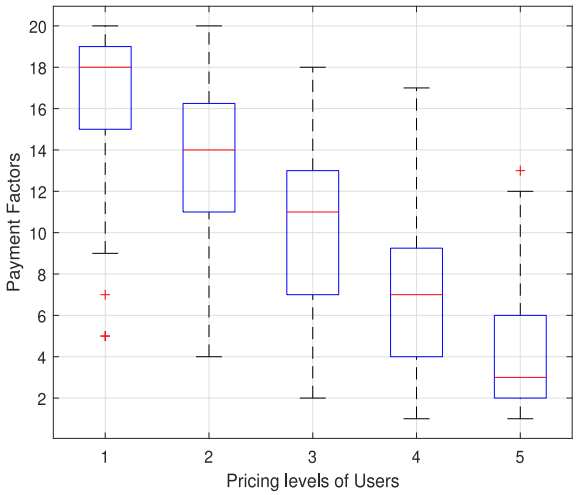


Fig. 3. Boxplot of the PF per pricing level of the combinations.

case, the optimization for computing the codebook entries is based on the NSGA-II algorithm [29]. This procedure generates a codebook entry for each user, consisting of 66 values for impedance capacitance. The impedance values range from 0.4 to 0.9 μF.

*6) PRIME Operation:* The PRIME algorithm retrieves the codebook entries from the Codebook Database and multiplexes them according to the PFs assigned to each user. For the sake of generality of the evaluation, 205 combinations of PFs are assigned to the users. (For the remainder, the term combination will refer to the set of PF values that are assigned to the users each time.) The assignment of the PFs is a random procedure. The values vary from 1 to 20. The PRIME uses a discretization parameter of 0.05 for the determination of the common RIS configuration, *CC*.

In Fig. 3, the values of the PF combinations are depicted. Users with higher PF values have an average PF of 16.8 with a standard deviation of 3.07, whereas users with lower PF values have an average PF of 4.8 with a deviation of 2.82. Within each combination, since no user shares the same PF value with another, five distinct pricing levels are formed.

The measurements of S21 for each user, once the RIS is set with *CC*, are computed for each combination of PFs. Since the use of PICCS ensures that the codebook entries include the optimal RIS configuration for serving each user individually, the performance for the allocation of RIS resources with

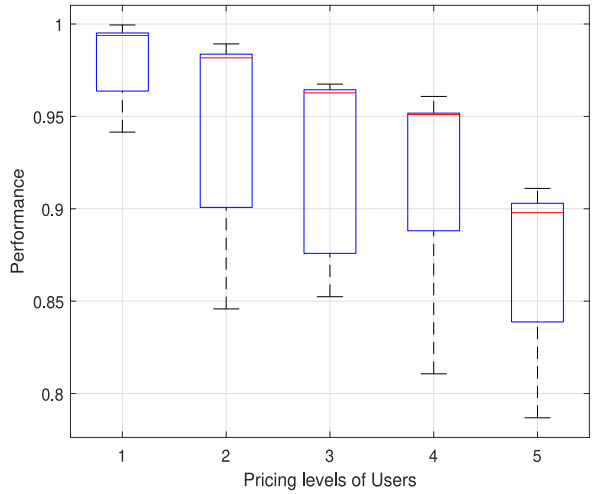


Fig. 4. Boxplot of the users' performance per pricing level with PRIME.

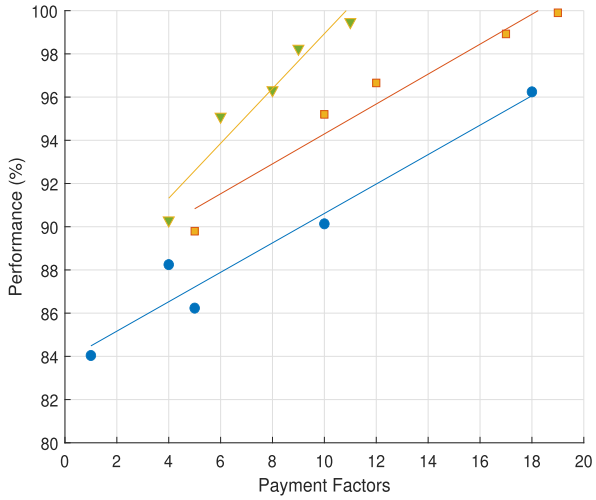


Fig. 5. The linear relationship between users' PF and performance with the usage of PRIME.

respect to user $k$ during combination $c$ is calculated as follows:

$$P_{kc} = \frac{S21_{opt_k} - S21_{kc}}{S21_{opt_k}} \tag{3}$$

The performance values for each user during the different combinations are depicted in Fig. 4. The average values for users, from highest to lowest, are 98%, 94%, 93%, 92%,and 87%, with variations of 2%, 5%, 4%, 3%, and 2%, respectively. As is evident, the measurements confirm that the PRIME can effectively allocate the RIS resources via the proper sharing of its elements for multiple users with different pricing levels.

### *B. Relationship Between PF and the Users' Performance Levels*

An aspect that requires further assessment is the relationship between each user's PF and their performance. PRIME offers a linear relationship between PF assigned to each user and the received performance [14]. This relationship is verified in Fig. 5. Specifically, three out of a total of 205 scenarios, each involving five users with varying PF values, are randomly selected and illustrated. It is evident that in all cases there is a linear proportionality between the assigned PF and the received performance.

The intercept of this line primarily represents the minimum efficiency level, indicating the performance that a basic user receives. The slope of the line denotes the performance enhancement achieved with the addition of each PF unit, as defined by telecommunication stakeholders. Accurate estimation of the intercept and slope in each network, combined with the PF assigned to each user, allows for easy approximation of their performance.

The intercept and the slope of PRIME's performance line are strongly influenced by the total number of users [14]. As a next step, we also investigate how the intercept and the slope are affected by the users' PF. This analysis aims to determine how the performance of a specific user with a given pricing level can be affected by the other users participating in the same network. To this end, we perform a correlation analysis

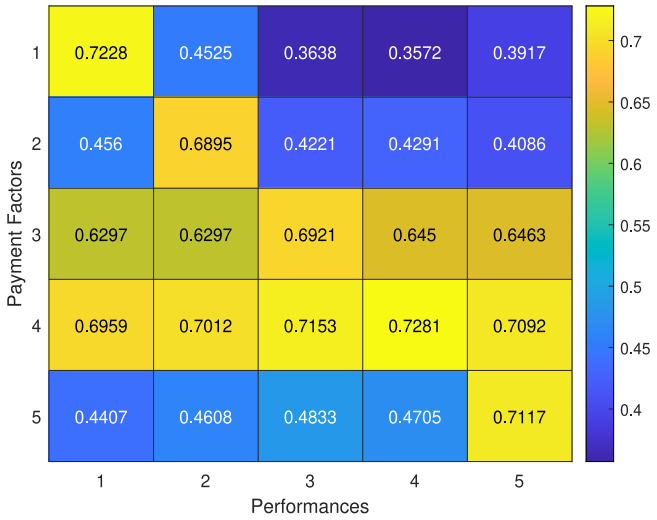


Fig. 6. The correlation matrix among all users' performance and PF values.

between the PF assigned to all users and the performance received by an individual user.

The correlation measures the strength and direction of the relationship between two variables, ranging from $-1$ (perfect negative correlation) to 1 (perfect positive correlation), with 0 indicating no correlation. As mentioned previously, no users have the same PF value in any combination. Therefore, we can shape five different pricing levels. Subsequently, we investigate the correlation between each PF value and the corresponding performance. The results are illustrated in Fig. 6.

The highest correlation is observed between each user group's PF values and their respective performance (major diagonal elements in Fig. 6). However, there is also a significant correlation with other PF user groups, ranging from 0.3572 to 0.7153. The highest correlations are seen in the groups with mid-level PF values, with a notable correlation greater than 0.6297, indicating a relatively strong relationship.

Having detected the correlation between user groups and performances, the objective analysis for intercept and slope

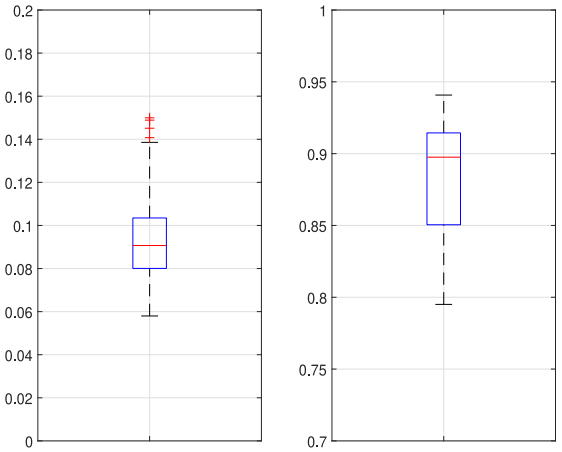


Fig. 7. Boxplot of the slope (left) and the intercept (right) of the performance line based on the PFs of the pricing levels.

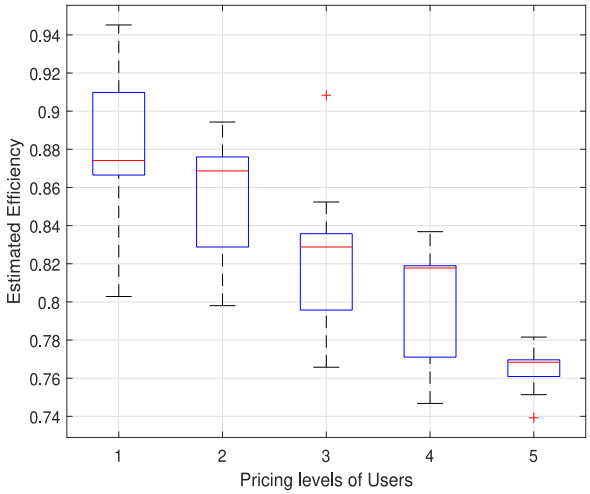


Fig. 8. Estimation of the RIS resource allocation achieved by PRIME.

of the performance line follows. For this task, we scale the PF values during each combination. Therefore, each scaled PF value is mapped in relation to the PF values of the rest users. After this action, each scaled PF is aligned with the respective performance, and the intercept and the slope factors are computed. The respective boxplot is illustrated in Fig. 7.

The mean value of the slope is 0.0928, with a standard deviation of 0.0185. For the intercept, the mean value is 0.8820, with a standard deviation of approximately 0.04. This indicates that PRIME ensures that all users can achieve performance levels between 84% and 92%, while users with higher PF values can approach 100% performance. A higher PF ensures that, irrespective of the PF values of the other users and the total number of them, the performance will be close to optimal.

### C. Evaluation via a Novel RIS Resource Allocation Efficiency Metric

In this section, we present a proposal for a metric to estimate the allocation efficiency for each user during the RIS resource sharing. This metric is based on the deviation between the configuration of the RIS elements when the user is served alone (codebook entry, *CE*) and the common RIS configuration $(CC)$, as calculated in Eq. (4).

$$D_k(i,j) \ = CE_k(i,j) \ - CC(i,j) \tag{4}$$

It has been shown that the deviation in each RIS element does not have the same effect on its macroscopic response [12]. For this reason, the metric also incorporates this physical aspect by computing the contribution of each deviation using Eq. (5).

$$AD_k(i,j) \ = D_k(i,j) \ \times Con(i,j) \tag{5}$$

The final efficiency per user is computed by subtracting 1 (the optimal case) from the sum of the resulting products of Eq. (5), as:

$$eff_k = 1 - Loss_k = 1 - \sum_{i,j} AD_k(i,j) \tag{6}$$

Having computed the accurate performance for each user, we use these measurements to evaluate the accuracy of the proposed metric. Using the same combinations for PF values, we also calculate the efficiency using this metric. The results are presented in Fig. 8.

The average efficiency, from higher to lower PF, is 88%, 86%, 82%, 80%, and 77%, with deviations of 5%, 4%, 3%, 3%, and 3%, respectively. Comparing Fig. 4 and Fig. 8, it is evident that the proposed metric has values approximately 8-11% lower than the actual performance values. This indicates that the proposed metric is a strict and reliable estimator for assessing the efficiency of any allocation method for RIS resources among multiple users with different pricing levels.

### D. Comparison of PRIME and COMMON

COMMON can multiplex codebook entries so that the same RIS unit can simultaneously serve multiple users. PRIME can accomplish the same task, but with the added capability of considering unique pricing levels for each user and assigning priorities accordingly. Essentially, COMMON can be viewed as a special case of PRIME where all users share the same pricing level.

To compare COMMON and LEVEL, we use the efficiency estimator from Section VI-C. We assume that a 100x100 RIS unit is serving 10 users simultaneously, with a discretization parameter of 0.05. As shown in Fig. 9, PRIME assigns PFs to each user incrementally, starting from 1 and increasing to 10 (with User ID=1 assigned PF=1, User ID=2 assigned PF=2, and so on). The codebook entries are simulated with varying values from 0 to 1 and for the multiplexing MATLAT is used.

Fig. 9 demonstrates that COMMON can effectively share the RIS by multiplexing codebook entries, resulting in an efficiency of approximately 57% for all 10 users. Regarding the PRIME algorithm and the associated sharing and pricing results, it is clear that the improved efficiency levels of high-PF users do not come at the expense of others, ensuring network fairness. The higher PF values can achieve efficiencies about 27% higher.

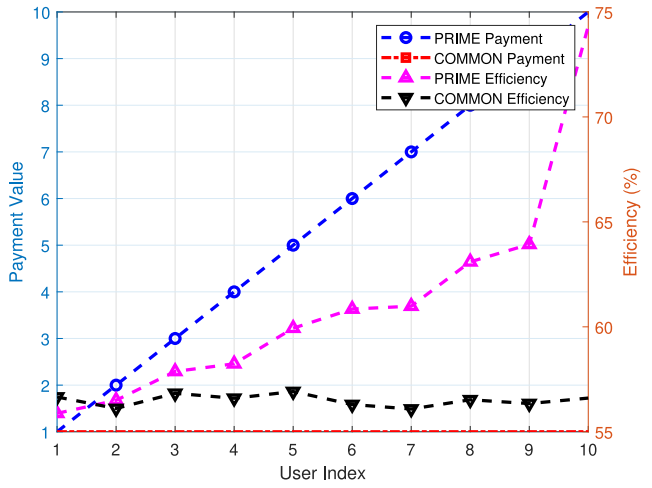


Fig. 9. User efficiency for PRIME and COMMON algorithms.

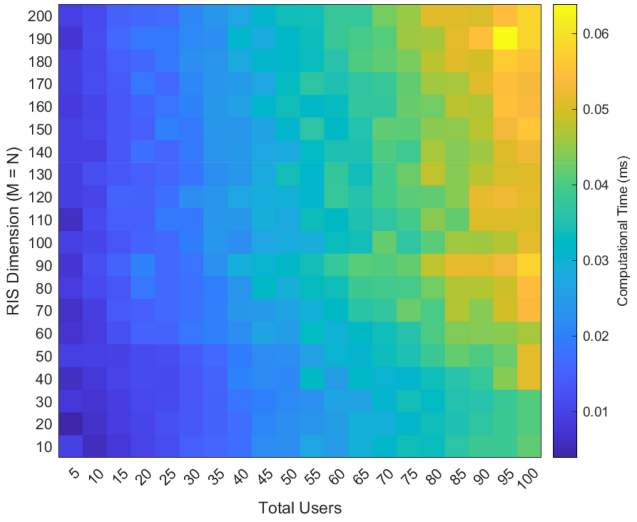


(a) COMMON algorithm.

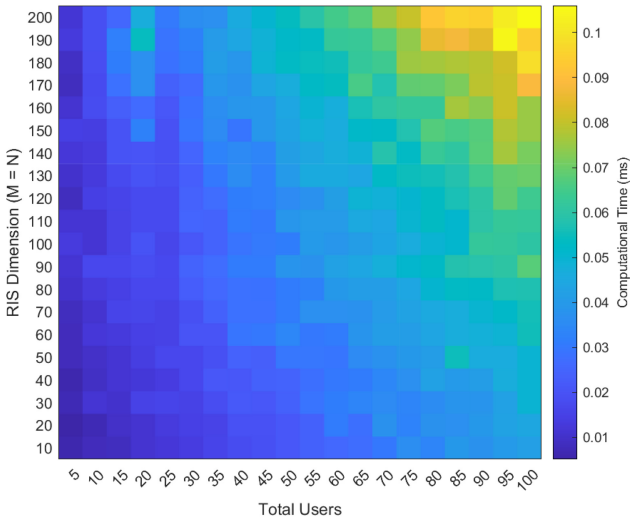


(b) PRIME algorithm.

Fig. 10. Heatmaps of the required computational time of COMMON (up) and PRIME (down) with respect to the total number of users and the RIS dimensions.

We also compared the computational time required by COMMON and PRIME. In this set of experiments, the number of users varies from 5 to 100, and the RIS dimensions range from $M = N = 10, 25, 50, .., 200$. In the PRIME algorithm, the PFs are randomly assigned values from 1 to 10. All computations are accelerated using a GPU unit. The results are presented in Fig.10(a) for COMMON and Fig.10(b) for PRIME.

Because of its workflow, the PRIME algorithm benefits significantly from GPU acceleration. As a result, the computational time required for PRIME is only about 40% greater than that required for COMMON. Even for very large RIS units serving many users, the computation time remains limited to approximately 0.1 ms. The ms-level latency of the PRIME renders it applicable also in dynamically changing network conditions, e.g., vehicular networks.

Furthermore, it is acknowledged that MATLAB is recognized for its relatively slower performance compared to other programming languages like C/C++ or Fortran. This underscores the practicality of the proposed algorithm in determining RIS configurations to efficiently serve multiple users with high RIS dimensions in realistic scenarios, particularly in terms of computational demands.

### *E. Resource Allocation in Cascaded-RIS Links*

In a realistic RIS-assisted environment, multiple RIS units are deployed to simultaneously serve numerous users. To manage this complexity, PRIME is utilized within each RIS unit to multiplex the users' *CE* to the *CC*.

We analyze three different cascaded scenarios:

1) Scenario 1: Five users are served by two RIS units.
2) Scenario 2: Five users are served within an environment consisting of five RIS units. Each user is served by a path that includes a subset of the RIS units.
3) Scenario 3: A crowded environment serves twenty users with fifty RIS units. Each user is served by a path that includes a subset of the RIS units.

In all scenarios, the RIS units are sized 50 x 50. PRIME assigns each user *PFs* ranging from 1 to 10. For each user-RIS pair, only the *CE* is essential. The number of transmitters in the network, as well as the communication protocol and frequency band, remain agnostic. The efficiency of each user in the cascaded scenarios is calculated as the average efficiency across the RIS units that comprise their path.

In the first scenario, the overall efficiency results for each user relative to their respective *PF* are illustrated in Fig. 11. PRIME functions effectively in this scenario.

Building on cascaded RIS links, we explore scenarios 2 and 3. We assign RIS units to users based on unique IDs, as depicted in Figs. 12(a) and 13(a). In these scenarios, another important factor to consider is the traffic in each RIS, which refers to the percentage of total users utilizing a specific unit. In the second scenario, where efficiency results are shown in Fig. 12(b), each RIS is utilized between 60% and 70%, with

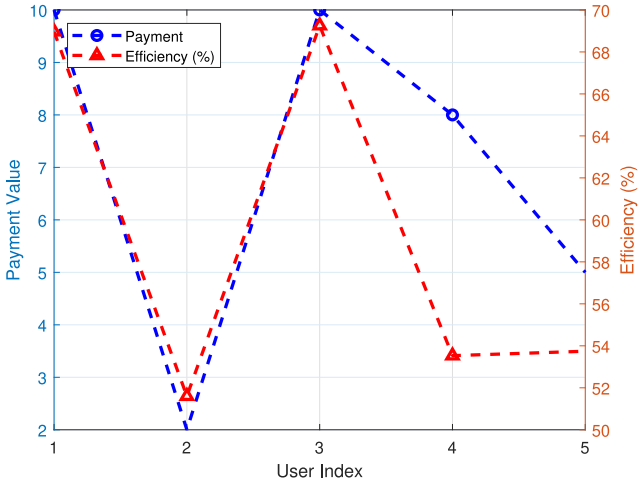


Fig. 11. The average efficiency of 5 users with 2 RIS units.

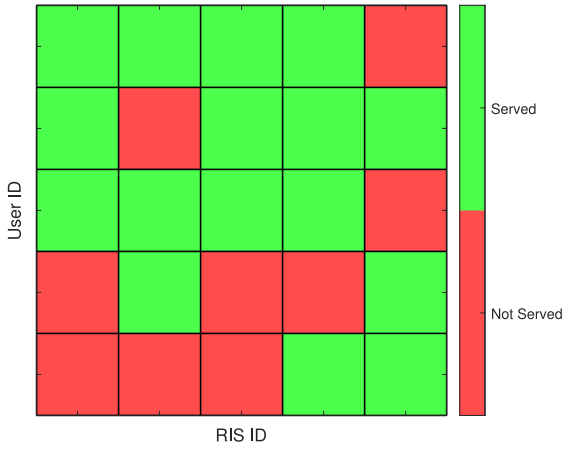


(a) Assignement of RIS units to users.

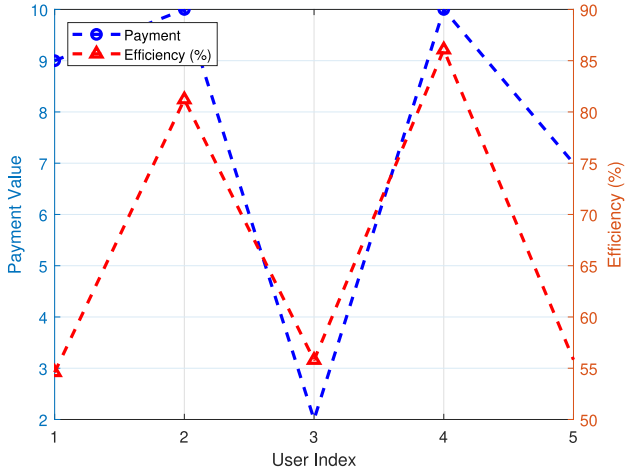


(b) Efficiency of each user.

Fig. 12. Cascaded RIS link with 5 users and 5 units.

RIS4 exhibiting the highest usage. In Scenario 3, traffic varies from 25% to 75%. Even in the most crowded case, users with higher *PF* maintain higher efficiency, as shown in the overall results in Fig. 13(b). Regarding computational performance,

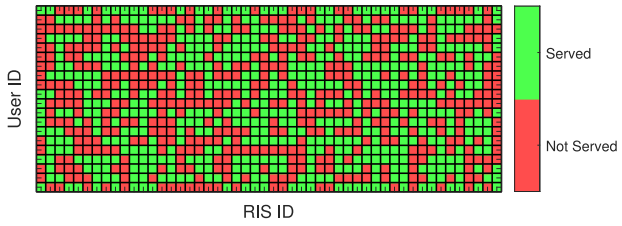


(a) Assignement of RIS units to users.

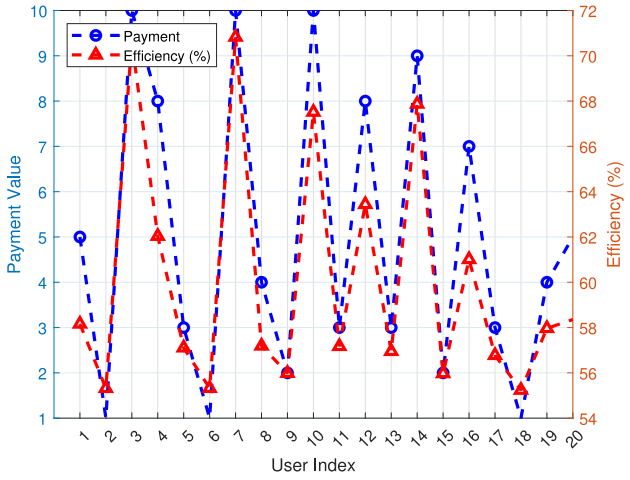


(b) Efficiency of each user.

Fig. 13. Cascaded RIS link with 20 users and 50 units.

the average time to calculate the *CC* across all cascaded links is 9 ms. In total, 523 computations were performed.

In conclusion, the PRIME method efficiently allocates resources and maintains high performance across various RIS-assisted scenarios involving cascaded-RIS links. It operates effectively under high traffic conditions, completing computations within milliseconds, which is sufficient for dynamic network environments.

## VII. Open Challenges

In this paper, we presented PRIME, the first algorithm dedicated to RIS resource allocation for users with different pricing levels, based on the multiplexing of codebook entries. The development of more algorithms aligned with the definition of the RIS as a network resource should continue, with these algorithms being evaluated against each other to establish the optimal solution in terms of performance and computational complexity.

These algorithms should focus on controlling the acceptable deviation between the individual codebook entries and the common RIS configuration. Furthermore, the cooperation of existing powerful metaheuristic tools should also be examined. Another topic to explore more is the case of a full PWE, where multiple RIS units exist in the network. The resource allocation of multi-hop communication links should be combined with the optimal path selection that ensures the fairness. In all these activities, the estimator proposed and evaluated in this paper could be utilized for accurate and fast computations.

An additional open challenge is leveraging the sharing ability of these algorithms to achieve more complex RIS functionalities. An indicative example of such functionality is beam splitting. In current approaches, beam splitting is treated as a complex optimization problem that tries to define the RIS configuration based on multiple users' positions. Instead, it could be addressed as a simple, pricing-based or not, multiplexing of various beam steering cases.

## VIII. Conclusion

In this paper, we define the notion of RIS as a share-able resource. This definition involves a mathematical procedure that aligns the sharing method of RIS elements to minimize the performance loss between the single-user scenario and the multi-user case. In this procedure, the pricing level of each user is used to assign a proportional weight.

Moreover, we propose and present PRIME, the first algorithm dedicated to pricing-based RIS resource allocation. We evaluate PRIME using full-wave electromagnetic simulations, which enhance the accuracy of the extracted results. We also discuss the linear relationship between each user's pricing level and their received performance. The computational complexity and required computational time in different scenarios indicate that PRIME can be effectively applied in real-world scenarios. PRIME has also been implemented in cascaded RIS links demonstrating sufficient efficiency in feasible for real-time usage computational time.

## Acknowledgment

The methodology was developed within WISAR and 6G-RIC, while NATWORK contributed to the experiments, key results, and conclusions.

## References

[1] C. Liaskos et al., "Software-defined reconfigurable intelligent surfaces: From theory to end-to-end implementation," *Proc. IEEE*, vol. 110, no. 9, pp. 1466–1493, Sep. 2022.

[2] C. Liaskos, S. Nie, A. Tsioliaridou, A. Pitsillides, S. Ioannidis, and I. Akyildiz, "A new wireless communication paradigm through software-controlled metasurfaces," *IEEE Commun. Mag.*, vol. 56, no. 9, pp. 162–169, Sep. 2018.

[3] J. Bae, W. Khalid, A. Lee, H. Lee, S. Noh, and H. Yu, "Overview of RIS-enabled secure transmission in 6G wireless networks," *Digit. Commun. Netw.*, vol. 10, no. 6, pp. 1553–1565, 2024.

[4] H. Zhang et al., "MetaRadar: Indoor localization by reconfigurable metamaterials," *IEEE Trans. Mobile Comput.*, vol. 21, no. 8, pp. 2895–2908, Aug. 2022.

[5] E. Basar, "Reconfigurable intelligent surfaces for doppler effect and multipath fading mitigation," *Front. Commun. Netw.*, vol. 2, May 2021, Art. no. 672857.

[6] C. Avin, K. Mondal, and S. Schmid, "Demand-aware network design with minimal congestion and route lengths," *IEEE/ACM Trans. Netw.*, vol. 30, no. 4, pp. 1838–1848, Aug. 2022.

[7] C. Liaskos, K. Katsalis, J. Triay, and S. Schmid, "Resource management for programmable metasurfaces: Concept, prospects and challenges," *IEEE Commun. Mag.*, vol. 61, no. 11, pp. 208–214, Nov. 2023.

[8] C. Liaskos and K. Katsalis, "A scheduling framework for performing resource slicing with guarantees In 6G RIS-enabled smart radio environments," *ITU J.*, vol. 4, no. 1, pp. 33–49, 2023.

[9] S. I. Raptis et al., "An accurate semi-analytical model for periodic tunable metasurfaces electromagnetic response," in *Proc. 18th Eur. Conf. Antennas Propag. (EuCAP)*, 2024, pp. 1–5.

[10] A. Lalas, N. Kantartzis, and T. Tsiboukis, "Programmable terahertz metamaterials through V-beam electrothermal devices," *Appl. Phys. A, Solids Surf.*, vol. 117, pp. 433–438, Aug. 2014.

[11] A. Li, S. Singh, and D. Sievenpiper, "Metasurfaces and their applications," *Nanophotonics*, vol. 7, no. 6, pp. 989–1011, 2018.

[12] A. I. Papadopoulos et al., "Physics-informed metaheuristics for fast RIS codebook compilation," *IEEE Commun. Mag.*, vol. 62, no. 11, pp. 152–158, Nov. 2024.

[13] M. Segata et al., "CoopeRIS: A framework for the simulation of reconfigurable intelligent surfaces in cooperative driving environments," *Comput. Netw.*, vol. 248, Jun. 2024, Art. no. 110443.

[14] A. Papadopoulos, A. Lalas, K. Votis, S. Schmid, K. Katsalis, and C. Liaskos, "RIS as a network resource: User multiplexing and pricing algorithms," in *Proc. 3rd Int. Conf. 6G Netw. (6GNet)*, 2024, pp. 144–152.

[15] A. Petrosino et al., "Dynamic management of forwarding rules in a T-SDN architecture with energy and bandwidth constraints," in *Proc. 19th Int. Conf. Ad-Hoc Netw. Wireless*, 2020, pp. 3–15.

[16] Y. Abiko, T. Saito, D. Ikeda, K. Ohta, T. Mizuno, and H. Mineno, "Flexible resource block allocation to multiple slices for radio access network slicing using deep reinforcement learning," *IEEE Access*, vol. 8, pp. 68183–68198, 2020.

[17] F. Fossati, S. Moretti, P. Perny, and S. Secci, "Multi-resource allocation for network slicing," *IEEE/ACM Trans. Netw.*, vol. 28, no. 3, pp. 1311–1324, Jun. 2020.

[18] I. Chang, T. Ji, R. Zhu, Z. Wu, C. Li, and Y. Jiang, "Towards an efficient and dynamic allocation of radio access network slicing resources for 5G era," *IEEE Access*, vol. 11, pp. 95037–95050, 2023.

[19] M. Leconte, G. S. Paschos, P. Mertikopoulos, and U. C. Kozat, "A resource allocation framework for network slicing," in *Proc. IEEE Conf. Comput. Commun.*, 2018, pp. 2177–2185.

[20] Z. Jahedi and T. Kunz, "Fast and cost-efficient virtualized network function placement algorithm in wireless multi-hop networks," in *Proc. 19th Int. Conf. Ad-Hoc Netw. Wireless*, 2020, pp. 23–36.

[21] Y. Zhang and H. Xu, "Optimal resource allocation for reconfigurable intelligent surface assisted dynamic wireless network via online reinforcement learning," in *Proc. IEEE Int. Conf. Sens., Commun., Netw. (SECON Workshops)*, 2022, pp. 13–18.

[22] P. S. Aung, L. X. Nguyen, Y. K. Tun, Z. Han, and C. S. Hong, "Deep reinforcement learning based joint spectrum allocation and configuration design for STAR-RIS-assisted V2X communications," *IEEE Internet Things J.*, vol. 11, no. 7, pp. 11298–11311, Apr. 2024.

[23] Y. Sun, F. Wang, and Z. Liu, "Coalition formation game for resource allocation in D2D uplink underlaying cellular networks," *IEEE Commun. Lett.*, vol. 23, no. 5, pp. 888–891, May 2019.

[24] Y. Zhang and H. Xu, "Two-stage online reinforcement learning based distributed optimal resource allocation for multiple RIS-assisted mobile ad-hoc network," in *Proc. Int. Conf. Comput., Netw. Commun. (ICNC)*, 2023, pp. 563–567.

[25] S. Lin, Y. Zou, J. Zhu, H. Guo, B. Li, and F. Xie, "Outage probability analysis of RIS-assisted wireless powered multi-user communications," in *Proc. 13th Int. Conf. Wireless Commun. Signal Process. (WCSP)*, 2021, pp. 1–5.

[26] *The Internet of Materials*. Boca Raton, FL, USA: CRC Press, 2020.

[27] M. Stănculescu et al., "Using s parameters in wireless power transfer analysis," in *Proc. 10th Int. Symp. Adv. Topics Elect. Eng. (ATEE)*, 2017, pp. 107–112.

[28] A. Papadopoulos et al., "An open platform for simulating the physical layer of 6G communication systems with multiple intelligent surfaces," in *Proc. 18th Int. Conf. Netw. Service Manage. (CNSM)*, 2022, pp. 359–363.

[29] S. Luke, *Essentials of Metaheuristics*, 2nd ed. Morrisville, NC, USA: Lulu, 2013. [Online]. Available: http://cs.gmu.edu/∼sean/book/metaheuristics/

**Alexandros Papadopoulos** received the Diploma degree in electrical engineering from the Aristotle University of Thessaloniki, Thessaloniki, Greece, in 2019. He is currently pursuing the Ph.D. degree with the Department of Computer Science and Engineering at the University of Ioannina, Ioannina, Greece. Since 2020, he has been employed as a Research Assistant with the Center for Research and Technology Hellas/Informatics and Telematics Institute, Thessaloniki. His primary research interests encompass 5G and beyond communication networks, V2X ecosystems, metasurfaces, and wireless channel engineering.

**Dimitrios Tyrovolas** (Member, IEEE) received the Diploma degree (five years) in electrical and computer engineering from the University of Patras, Greece, in 2020, and the Ph.D. degree from the Department of Electrical and Computer Engineering, Aristotle University of Thessaloniki, Greece, in 2024. Since 2024, he has been a Postdoctoral Fellow with the Wireless Communications and Information Processing Group, Aristotle University of Thessaloniki, Thessaloniki, Greece. He is also a Research Assistant with Dienekes SI IKE, Heraklion, Greece. His current research interests include reconfigurable networking, reconfigurable intelligent surfaces, pinching-antenna systems, and UAV communications. He was an exemplary Reviewer of IEEE *Wireless Communications Letters* in 2021, and IEEE COMMUNICATIONS LETTERS in 2022 (top 3% of reviewers).

**Antonios Lalas** received the Ph.D. degree in electrical and computer engineering in 2012. From 2012 to 2018, he was an Adjunct Lecturer with the Department of Informatics and Telecommunications Engineering, University of Western Macedonia (UOWM). He was a Postdoctoral Research Fellow with ECE AUTH from 2013 to 2015. From 2020 to 2021, he was an Adjunct Lecturer with the Department of ECE, UOWM. He is currently a Postdoctoral Researcher with the Information Technologies Institute/Centre for Research and Technology Hellas (CERTH/ITI). He has also been involved in several research projects, such as NATWORK, ARROW (6G-SANDBOX OC1), SWARMCATCHER (FIDAL OC1), AUTOTRUST, where he serves as the deputy-coordinator. His research interests include 5G/6G networks, V2X communications, artificial intelligence, reconfigurable intelligent surfaces, metamaterials, IoT in autonomous vehicles, counter-UAV, (cyber-)security, and eHealth domains.

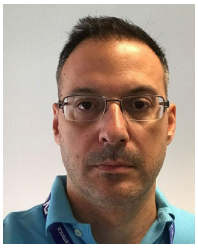

**Konstantinos Votis** received the M.Sc. and Ph.D. degrees in computer science and service-oriented architectures, and the M.B.A. degree from the Business School Department, University of Patras, Greece. He is currently a Computer Engineer and a Senior Researcher (Researcher Grade B') with the Information Technologies Institute/Centre for Research and Technologies Hellas (CERTH/ITI), where he is the Director of the Visual Analytics Laboratory. He has been also a Visiting Professor with the Institute of the Future, University of Nicosia, regarding blockchain and AI technologies since October 2019. He was also a Visiting Professor of Human Computer Interaction, Virtual and Augmented Reality with the De Montfort University, U.K., from 2016 to 2020. His research interests include human computer interaction, information visualization and management of big data, knowledge engineering, and decision support systems.

**Stefan Schmid** received the M.Sc. and Ph.D. degrees from ETH Zürich. He is a Professor with the Technical University of Berlin, Germany. He was a Postdoctoral Fellow with TU Munich and the University of Paderborn, a Senior Research Scientist with T-Labs, Berlin, an Associate Professor with Aalborg University, Denmark, a Full Professor with the University of Vienna, Austria, and Sabbathical as a Fellow with the Israel Institute for Advanced Studies, Israel. He received the IEEE Communications Society ITC Early Career Award in 2016 and an ERC Consolidator Grant 2019.

**Sotiris Ioannidis** received the B.Sc. degree in mathematics and the M.Sc. degree in computer science from the University of Crete in 1994 and 1996, respectively, and the Ph.D. degree from the University of Pennsylvania in 2005. He was a Research Director with FORTH until 2020. He is currently an Professor with the Technical University of Crete and the Director of the Microprocessor and Hardware Laboratory.

**George K. Karagiannidis** (Fellow, IEEE) is currently a Professor with the Electrical and Computer Engineering Department, Aristotle University of Thessaloniki, Greece, and the Head of Wireless Communications and Information Processing Group. He is also a Visitor Professor with Taif University, Taif, Saudi Arabia. His research interests are in the areas of wireless communications systems and networks, signal processing, optical wireless communications, wireless power transfer and applications, and communications and signal processing for biomedical engineering. Recently, he received three prestigious awards: The 2021 IEEE ComSoc RCC Technical Recognition Award, the 2018 IEEE ComSoc SPCE Technical Recognition Award, and the 2022 Humboldt Research Award from Alexander von Humboldt Foundation. He is one of the highly-cited authors across all areas of Electrical Engineering, recognized from Clarivate Analytics as Web-of-Science Highly-Cited Researcher from 2015 to 2024. He is the Editor-in Chief of IEEE TRANSACTIONS ON COMMUNICATIONS and in the past was the Editor-in Chief of IEEE COMMUNICATIONS LETTERS.

**Christos K. Liaskos** received the Diploma degree in electrical engineering from the Aristotle University of Thessaloniki (AUTH), Greece, in 2004, the M.Sc. degree in medical informatics from the Medical School, AUTH in 2008, and the Ph.D. degree in computer networking from the Department of Informatics, AUTH in 2014. He is currently an Assistant Professor with the University of Ioannina, Ioannina, Greece, and an Affiliated Researcher with the Foundation for Research and Technology Hellas (FORTH), Heraklion, Greece. His research interests include computer networks, traffic engineering, and novel control schemes for wireless communications.